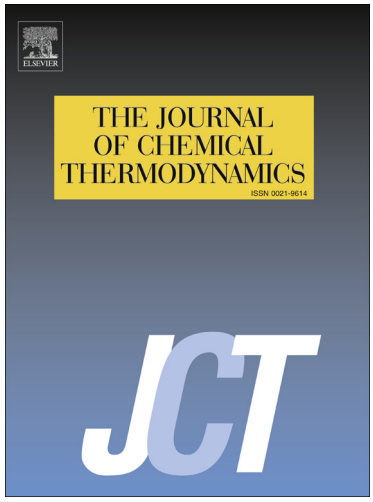

Kinetics of the solid-solid transformations for the Piracetam Trimorphic system: incidence on the construction of the p-T equilibrium phase diagram

Yohann Corvis, Anne Spasojević-de Biré, Camille Alzina, Nicolas Guiblin, Philippe Espeau

PII: S0021-9614(16)00033-1
DOI: http://dx.doi.org/10.1016/j.jct.2016.01.016
Reference: YJCHT 4531

To appear in: *J. Chem. Thermodynamics*

Received Date: 2 June 2015
Revised Date: 5 January 2016
Accepted Date: 22 January 2016

Please cite this article as: Y. Corvis, A.S-d. Biré, C. Alzina, N. Guiblin, P. Espeau, Kinetics of the solid-solid transformations for the Piracetam Trimorphic system: incidence on the construction of the p-T equilibrium phase diagram, *J. Chem. Thermodynamics* (2016), doi: http://dx.doi.org/10.1016/j.jct.2016.01.016

Kinetics of the solid-solid transformations for the Piracetam Trimorphic system: incidence on the construction of the p-T equilibrium phase diagram

Yohann Corvis,[ab] Anne Spasojević-de Biré,[cd] Camille Alzina,[a] Nicolas Guiblin[cd] and Philippe Espeau[*ab]

[a] Former affiliation: EA 4066 « Physico-Chimie Industrielle du Médicament », Faculté des Sciences Pharmaceutiques et Biologiques, Université Paris Descartes, 4 Avenue de l'Observatoire, 75 006 Paris, France.

[b] Unité de Technologies Chimiques et Biologiques pour la Santé, UMR8258 CNRS, U 1022 INSERM. Faculté des Sciences Pharmaceutiques et Biologiques, Université Paris Descartes, 4 avenue de l'Observatoire, 75 006 Paris.

[c] CentraleSupélec, Grande Voie des Vignes, 92 295 Châtenay-Malabry, France.

[d] CNRS, UMR 8580, Laboratory "Structures Propriétés et Modélisation des Solides" (SPMS), Grande Voie des Vignes, 92 295 Châtenay-Malabry, France.

*** Corresponding author.** Unité de Technologies Chimiques et Biologiques pour la Santé, UMR8258 CNRS, U 1022 INSERM. Faculté des Sciences Pharmaceutiques et Biologiques, Université Paris Descartes, 4 avenue de l'Observatoire, 75 006 Paris. Ph/fax: +33 (0) 1 53 73 96 76. E-mail address: philippe.espeau@parisdescartes.fr

Abstract

The three common polymorphs of piracetam have been characterized by associating thermal analysis, X-ray diffraction and densimetry. DSC experiments showed that the solid-solid transition temperature between Forms II and I and between Forms III and I is scan-rate dependent. The transition temperatures decrease when the DSC scan rate decreases and the thermodynamic temperatures were confirmed by isothermal X-ray diffraction.

These new results in terms of temperature and enthalpy of transition allow us to propose a new equilibrium phase diagram establishing the relative thermodynamic stability of the three common polymorphs of piracetam as a function of the temperature and the pressure.

The diagram suggests that Form II presents a small stability domain located just above the stability domain of Form I. As a consequence, Form I should transform into Form II, which itself can turn into Form III when placed under pressure.

Keywords: Piracetam, Polymorphism, Calorimetry (DSC), X-ray diffractometry, Thermodynamics, Physical stability.

1. Introduction

Piracetam, $C_6H_{10}N_2O_2$, is a nootropic drug whose chemical name is 2-oxo-1-pyrrolidine acetamide (scheme 1). It is used as adjunctive therapy against chronic pathological cognitive and neurosensory deficits. This drug is usually administered in solid form.

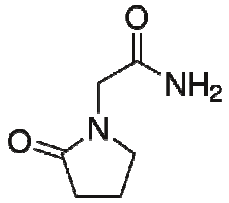

Scheme 1: chemical structure of piracetam.

No less than five polymorphs of this substance have been characterized and subsequently reported in the literature [1-8]. The most commonly studied polymorphic forms are referenced as I, II and III. The first solid form crystallizes in a monoclinic lattice and is the stable form at high temperature [3-7, 9-11]. Its melting point is ~ 435 K. The second and the third polymorphs are reported to crystallize in triclinic and monoclinic systems, respectively [2]. Throughout the literature, there is some conflicting evidence about the stability hierarchy of Forms II and III. However, Form III is the usual commercial sample and this could suggest that this form is the thermodynamically most stable phase under normal conditions of temperature and pressure, as attested by former studies [3,5-11]. However, a previously reported state diagram of piracetam revealed that, due to a measured III-I transition temperature lower than that of the II-I, Form II was the most stable form at ordinary pressures [4]. Moreover, the authors claimed that Form III was a high-pressure phase and that form II could transform into Form III under increased pressure. This statement is thus in contradiction with the fact that Form III was proven to be the most stable form under normal conditions. On this basis, one may wonder what the exact stability hierarchy between Forms II and III is, taking into account the temperature and the pressure effect.

Forms IV and V have been described as high-pressure polymorphs [3,6]. Form IV was obtained by crystallization under high pressure and structurally characterized by *in situ* high-pressure X-ray diffraction [5]. According to these authors, when decreasing the pressure, Form IV undergoes a polymorphic transformation into Form II. As far as Form V was concerned, it was obtained by direct compression of Form II and structurally characterized by *in situ* high-pressure X-ray diffraction [6]. On decreasing the pressure, Form V reversibly transforms into Form II. As for Form IV, no data, such as temperature and enthalpy of transition and/or melting, are available.

In the present paper, thermal analyses are coupled with isothermal X-ray diffraction to provide new thermodynamic data regarding the piracetam solid-solid transitions, which are proven to be kinetically-dependent. From these new results, new thermodynamic relative stabilities between the three polymorphs I, II and III of piracetam are established as a function of temperature and pressure. This thermodynamic approach describes the equilibrium states between these three polymorphs in a two-dimensional space where pressure and temperature are used as variables. The knowledge of the p-T phase diagram of a substance is particularly

important for drugs since external pressure exerted on a drug during tableting may result in polymorphic transformations as well as in changes of physico-chemical properties [12].

2. Experimental

2.1. Chemicals

Piracetam was obtained from Sigma (purity higher than 99.5%) and was used without further purification. N-octadecane with a purity higher than 99% was purchased from Alfa-Aesar. Table 1 reports the purities stated by the supplier for all the the materials used in this work.

TABLE 1 Sample purity description.

Component	Source	Mass fraction Purity from supplier	Purification method
Piracetam	Sigma	> 0.995	None
N-octadecane	Alfa-Aesar	> 0.99	None
Indium	Mettler-Toledo	> 0.99999	None
Zinc	Mettler-Toledo	> 0.99998	None

2.2. Thermal analysis

The differential scanning calorimetry experiments were performed using an 822e thermal analyzer from Mettler-Toledo (Switzerland). Indium and zinc (purity higher than 99.9%, table 1), from Mettler-Toledo, were used for temperature and enthalpy calibration of the DSC device. For all the experiments, an empty aluminum pan was used as a reference. The DSC experiments were carried out at different scan rates from 0.1 to 10 °C min^{-1} in the 300-450 K temperature range. Each transition temperature was determined at the onset of the corresponding thermogram signal. Sample masses around 10 mg were used for each experiment and measured with an analytical balance (Mettler Toledo, Switzerland) with an accuracy of ± 0.01 mg.

2.3. X-ray powder diffraction

X-ray data collection was performed on a home-made diffractometer with a Rigaku RA-HF18 rotating anode generator (50 kV, 300 mA). The home-made goniometer was set as previously described [13]. Monochromatic Cu Kα1 (λ = 1.54056 Å) radiation was selected by means of a nickel filter. The sample was placed on a cryofurnace (TBT - Air Liquide) with a temperature range between -190 and 210 °C, using liquid nitrogen. Each data scan was

recorded between 5 and 60° in 2θ, with a step of 0.02° and a counting time of 1 second per step.

The cryofurnace was calibrated in temperature using a powder sample of Y_2O_3 for which the lattice parameters are known as a function of the temperature [14]. Then, for a given set temperature, the lattice parameters were refined and compared to the lattice parameters obtained at the true temperature. The standard uncertainty on the temperature is estimated to be 0.1 °C.

Cell parameters were obtained by pattern matching using JANA2006 sofware [15].

2.4. Liquid molar volumes

The molar volume of liquid piracetam was determined as a function of the temperature with a DMA-4500 densimeter coupled with a DMA HP density-measuring cell from Anton-Paar (Austria). Data were collected from 420 to 473 K. The standard uncertainty on the temperature is estimated at 0.01 °C. The period oscillation of the measurement cell of the densimeter was calibrated using two reference samples, namely dry air and n-octadecane, as a function of temperature.

3. Results and discussion

3.1. Transition points determination

The commercial sample was first characterized by X-ray powder diffraction (XRPD) performed at 300K. The experimental XRPD pattern was found to fit with that of Form III [2], calculated from single crystal data at 300 K (table 2).

TABLE 2 Lattice parameters for the three piracetam polymorphs obtained from experimental powder diffraction (this work and from ref. [8]) and single crystal refinements from ref. [2, 8].

	I		II		III	
	Monoclinic $P2_1/n$ Z = 4		Triclinic $P\bar{1}$ Z = 2		Monoclinic $P2_1/n$ Z = 4	
T (K)	300	400	300	300	300	300
Ref.	8	This work	2	This work	2	This work
A (Å)	6.747±0.002	6.773±0.002	6.403±0.003	6.3899±0.0011	6.525±0.002	6.5114±0.0011
b (Å)	13.418±0.003	13.532±0.004	6.618±0.004	6.6060±0.009	6.440±0.002	6.4300±0.0013
c (Å)	8.090±0.002	8.157±0.003	8.556±0.006	8.5415±0.0013	16.463±0.005	16.442±0.003
α (°)			79.85	79.813± 0.00		
β (°)	99.01±0.003	99.475±0.010	102.39±0.03	102.430±0.009	92.19±0.03	92.026±0.009
γ (°)			91.09±0.03	88.933±0.008		
V ($Å^3$)	723.36	737.3±0.4	348.51±0.02	346.17±0.09	691.29±0.06	688.0±0.2
d (g cm^{-3})	1.306	1.281±0.001	1.356	1.365±0.001	1.366	1.373±0.001

The estimated uncertainties on the lattice parameters are standard uncertainties. The standard uncertainty on the temperature is estimated at u(T) = ± 0.1 K.

Form III was then heated by DSC at different scan rates from 0.1 to 10 °C min^{-1}. It was observed that Form III transformed into Form I (figure 1, curve a) at a temperature decreasing from 123.7 °C at 10 °C min^{-1} to 100.9 °C at 0.1 °C min^{-1} (table 3). XRPD experiments were performed as a function of the temperature from 27 °C (300 K) to 147 °C (420 K) with a 24-hour acquisition time for a given temperature. We observed that Form I began to appear at 97 °C. This value has to be considered as the thermodynamic transition temperature corresponding to the DSC value when scan rate tends to zero.

Randomly, for some experiments carried out by DSC on Form III at 10 °C min^{-1}, we get a transformation of Form III at a higher temperature (Figure 1, curve b). This could not be ascribed to a transformation into Form I, the latter occurring at a lower temperature. We therefore hypothesized that this transformation could be the Form III toward Form II transformation, followed by the melting of Form II and recrystallization into Form I.

Interestingly, a direct melting of Form III has been randomly observed by DSC (Figure 1 curve c), as previously reported [4], making it possible to determine melting temperature and enthalpy for this polymorph (table 4).

When Form I is quenched at room temperature and immediately heated at 10 °C min^{-1}, a direct melting is sometimes obtained, as shown in Figure 1 curve d.

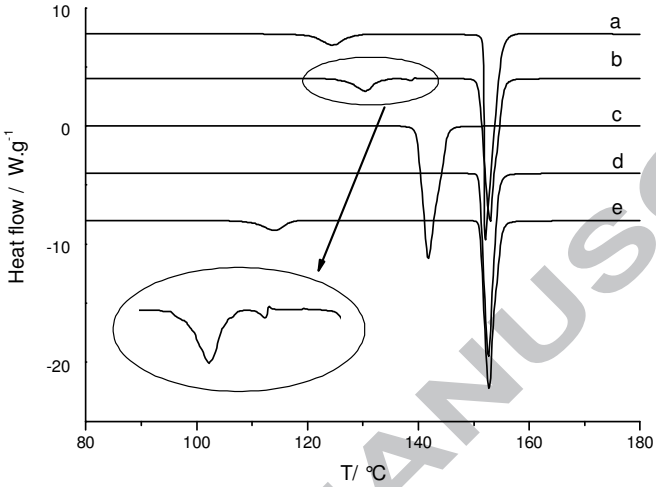

FIGURE 1. DSC curves of piracetam obtained upon heating at 10 °C min^{-1}. (a) Form III transformation into Form I before melting, (b) Form III transformation into Form II followed by melting - recrystallization into Form I (*cf.* the inset), (c) Direct melting of Form III, (d) Direct melting of Form I, (e) Form II transformation into Form I before melting. Endothermic transformations are pointed down.

TABLE 3 Temperature of transition points (triple points) III-I and II-I of piracetam as a function of the DSC heating rate. For both transition points, the vapor phase is in equilibrium with the solids at the given transition temperature.

V (°C min^{-1})	T_{III-I} (°C)	T_{II-I} (°C)
0.1	100.9	91.9
0.2	100.8	92.5
2	106.95	97
5	111.2	107
10	123.7	109.7

Standard uncertainty on the temperature is estimated at: u(T) = ± 2.5 °C

TABLE 4 Experimental piracetam triple points compared to the published data (for each transition point, the vapor phase has to be considered as the third phase in equilibrium at the triple points).

transition	T / °C	ΔH / J g^{-1}	method	Ref.
II → I	≈75	22.1	Thermomicroscopy	3
	125.8	24	DSC (10 °C min^{-1})	4
	109.5	22.7	DSC (5 °C min^{-1})	7
	109	23.7	DSC (50 °C min^{-1})	10
	~ 90	23.9	Ex-situ XRD	11
	91.9	24.8	DSC (extrapolation at 0 °C min^{-1})	This work
	87		XRPD (static)	
III → I	≈120	26.7	Thermomicroscopy	3
	118.8	28	DSC (10 °C min^{-1})	4
	121.2	26.2	DSC (5 °C min^{-1})	7
	120	26.5	DSC (50 °C min^{-1})	10
	~ 95	26.7	Ex-situ XRD	11
	100.9	26.8	DSC (extrapolation at 0 °C min^{-1})	This work
	97		XRPD (static)	

III → liq	140.2	206.1	DSC (5 °C min^{-1})	3
	138.8	210	DSC (10 °C min^{-1})	4
	135 and 149		Estimated from solubility data	10
	138.3		DSC (5 °C min^{-1})	11
	139.4(DSC)	211.3	DSC (10 °C min^{-1})	This work
II → liq	140.5	201.9*	DSC (5 °C min^{-1})	3
	142	204*	DSC (10 °C min^{-1})	4
	136 and 153		Estimated from solubility data	10
	139		DSC (5 °C min^{-1})	11
	141.5*			This work
I → liq	≈153	180.8	DSC (5 °C min^{-1})	3
	152.8	180	DSC (10 °C min^{-1})	4
	151.3	182.9	DSC (5 °C min^{-1})	7
	150		DSC (50 °C min^{-1})	10
	150	179.3	DSC (5 °C min^{-1})	11
	149.8(DSC)	187	DSC (10 °C min^{-1})	This work

* calculated value

Standard uncertainties are estimated as follows: u(T) = ± 2.5 °C for DSC experiments, u(T) = ± 3 °C for static XRPD experiments, u(ΔH) = ± 3 kJ mol^{-1} for II-I and III-I solid-solid transitions, and u(ΔH) = ± 2 kJ mol^{-1} for III-liq and I-liq melting points.

Form II was obtained either by recrystallization into isopropanol or by heating Form III to 140 °C in order to obtain Form I and then annealing at room temperature (RT) for three days. We observed by XRPD that Form II remained stable at room temperature for several hours. The XRPD pattern of Form II obtained at 300 K was compared to the profile obtained from the crystal structure performed at 300 K (table 2). As for Form III, piracetam Form II was heated at different DSC scan rates from 0.1 to 10 °C min^{-1}. Upon heating, Form II transformed endothermally into Form I at a temperature which is also function of the heating rate. The transition temperature decreased from 109.7 °C, obtained for a scan rate of 10 °C min^{-1} (Figure 1 curve e) to 91.9 °C at 0.1 °C min^{-1} (table 3). A temperature of 87 °C was deduced from the isothermal X-ray diffraction experiments (table 4). As a result, Form II

transformed into Form I at a temperature always lower than the III → I transition temperature. This statement is in agreement with most of the published articles [3, 7, 11] but in contradiction with another one [4].

The two solid-solid transition temperatures obtained from our XRPD experiments on pure piracetam, III-I and II-I, agree with the values deduced from XRD analysis of binary mixtures of piracetam and 1,4-dioxane [11].

As far as Form I is concerned, the X-ray powder pattern was performed at 130 °C, a temperature at which this polymorph is stable. The pattern was compared to the X-ray powder previously obtained at room temperature (table 2) [8]. From the DSC experiments, it was shown that Form I melting point is not scan rate-dependent. This suggests that the product does not degrade significantly on melting. Otherwise, the melting temperature would have increased with increasing the scanning rate, as was previously reported for vitamin C [16].

All the results regarding the piracetam experimental transition data are gathered in table 3.

When Form I is quenched and annealed at room temperature for one day, it is transformed into Form II and, after 1 month, Form II is completely transformed into Form III. This goes along with the fact that this is not the most stable form that usually crystallizes first but the least stable polymorph, as stated by Ostwald's rule [17].

Molar volumes of the three solid forms, as well as that of molten piracetam, were determined as a function of the temperature (table 5 and figure 2). The experimental points were fitted with a linear regression and the results are reported in table 6. This allowed us to conclude that Form III is always denser than Form II throughout the 275-360 K temperature range, *i.e.* up to the stability domain of Form I. This implies that Form III is the most stable polymorph in this range of temperature (by applying the density rule) [18]. The molar volumes of molten piracetam are measured with increasing temperature. As can be seen in figure 2, the linearity of the experimental points corroborates the non-degradation of piracetam in the molten state, at least up to 480 K.

TABLE 5 Experimental molar volumes (in cm^3 mol^{-1}) for piracetam in the solid and liquid states obtained from XRPD and liquid density measurements, respectively.

T (K)	Form III	Form II	Form I	Liquid
300	103.58	104.23		
310	103.13	104.41		
320	103.85	104.50		
330	103.60	104.93		
340	104.25	105.07		
350	104.20	105.40		
355		105.40		
360	104.69	105.45		
370	104.85		110.41	
375			110.54	
380			110.60	
385			110.77	
390			110.84	
395			110.98	
400			111.00	
405			111.19	
410			111.21	
423				122.82
428				123.15
433				123.47
438				123.85
443				124.14
448				124.51
453				124.83
458				125.20
463				125.54
468				125.89
473				126.24

Standard uncertainties are estimated as follows: u(T) = ± 0.1 K, u(V/m, solid) = ± 0.24 cm^3 mol^{-1}, u(V/m, liquid) = ± 0.22 cm^3 mol^{-1}.

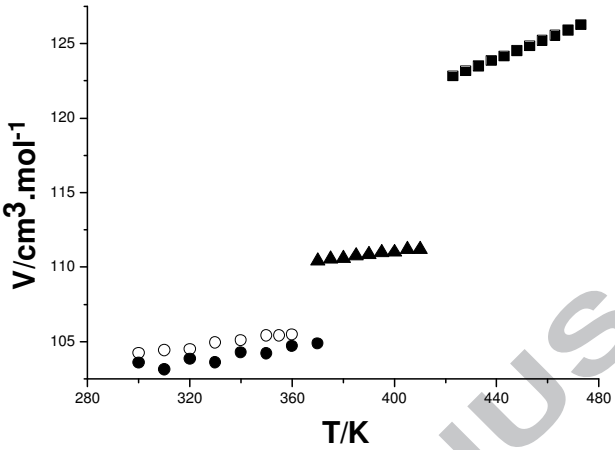

FIGURE 2. Piracetam molar volumes in the solid and liquid states. (●) Form III, (○) Form II, (▲) Form I, and (■) liquid.

TABLE 6 Regression coefficients for piracetam molar volumes of the three solid forms I, II and III, and the liquid state, V (cm^3 mol^{-1}) = a.T/K + b, and their corresponding standard deviations.

	III	II	I	liquid
a (cm^3 mol^{-1} K^{-1})	0.02189 ± 0.0040	0.0221 ± 0.0014	0.0205 ± 0.0009	0.0685 ± 0.0004
b (cm^3 mol^{-1})	96.68 ± 1.34	97.57 ± 0.48	102.86 ± 0.38	93.85 ± 0.15
r^2	0.91317	0.98758	0.99233	0.9999

The melting point of Form II had never been observed experimentally. To have access to the temperature and enthalpy of melting of this polymorph, we carried out Hess cycles [19] taking into account the II-I transition point and the melting data of Form I. Then, assuming that the Cp variations are negligible in the considered temperature range, we get:

$$\Delta_{fus}H(II, T_{fus}(II)) = \Delta_{fus}H(I, T_{fus}(I)) + \Delta_{trans}H(II-I, T_{trans}(II-I)) \quad (1)$$

Thus: $\Delta_{fus}H(II, T_{fus}(II)) = =211.8$ J g^{-1}

This value is slightly higher than the melting enthalpy of Form III, maybe because the calculated value is overestimated. A higher value of $\Delta_{fus}H(II)$ compared to $\Delta_{fus}H(III)$ would contradict the fact that Forms III and II are enantiotropically related [11]. Indeed, for a pair of polymorphs enantiotropically related, the melting enthalpy of the polymorph with the higher melting point has to be less than that of the polymorph with the lower melting point [20]. But, in fact, we will see below that the overestimated value of $\Delta_{fus}H(II)$ will not alter the further calculations and conclusions.

Regarding the entropy variation, we can also apply that:

$$\Delta_{fus}S(II, T_{fus}(II)) = \Delta_{fus}S(I, T_{fus}(I)) + \Delta_{trans}S(II-I, T_{trans}(II-I)) \quad (2)$$

Thus:

$$\frac{\Delta_{fus}H(II, T_{fus}(II))}{T_{fus}(II)} = \frac{\Delta_{fus}H(I, T_{fus}(I))}{T_{fus}(I)} + \frac{\Delta_{trans}H(II-I, T_{trans}(II-I)}{T_{trans}(II-I)})$$

From the values reported in table 3 and the calculated enthalpy of melting of Form II, we obtain: $T_{fus}(II) =$ 414.5 K = 141.5 °C, in agreement with previously reported values [3,4].

3.2. Determination of the phase diagram

Taking into account the new determined data of temperature and enthalpy of transition (solid-solid and solid-liquid) for the three polymorphs, a new phase diagram of pressure versus temperature of the piracetam system can be established in order to get some insight about the relative stability of the three polymorphs.

The effect of the pressure on the transition points (solid-solid or solid-liquid) can be evaluated using the Clapeyron equation [21-23]. The changes of the molar volume ΔV at the transition points were obtained from the plots of figure 2 at the corresponding transition temperature. The resulting slopes of the two-phase equilibrium curves are then given in table 7.

TABLE 7 Molar volume jumps at transition points (stable and metastable (*)) for piracetam, determined at the transition temperature and the calculated slopes of the two-phase equilibrium curves. In each case, the vapor phase is in equilibrium with the two phases coexisting at the given transition temperature.

	T (K)	ΔV (cm^3 mol^{-1})	dP/dT (MPa K^{-1})
II-I*	360	4.71	2.08
III-I	370	6.18	1.67
III-liquid*	412.4	16.97	4.29
II-liquid*	414.5	16.59	4.38
I-liquid	422.8	11.29	5.57

Standard uncertainty on the temperature is estimated at $u(T) = \pm 2.5$ K and the relative standard uncertainties as follows: $u_r(\Delta V) = 0.1\ \Delta V$, $u_r(dP/dT) = 0.02\ dP/dT$

Although the melting points of Forms II and III are very close, all authors agree to say that $T_{fus}(III) < T_{fus}(II) < T_{fus}(I)$ [3,4,11]. These points are, from a thermodynamic point of view, triple points, where the solid phase is in equilibrium with the liquid phase and the vapor phase. As a consequence, those three triple points share the same liquid-vapor equilibrium curve in the p-T plane (points 1 to 3 in Figure 3).

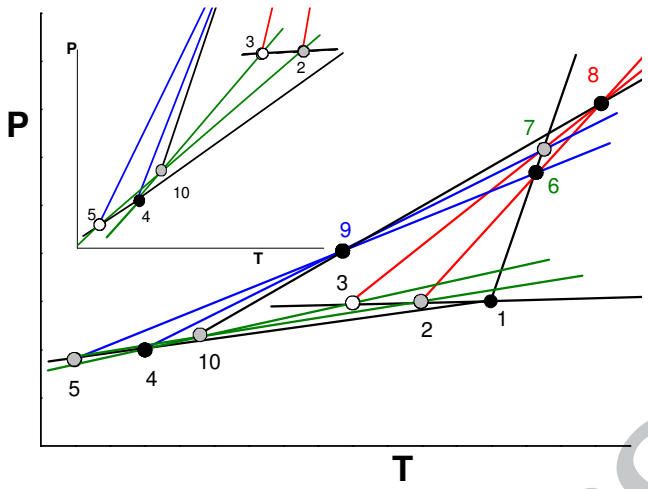

FIGURE 3. Schematic pressure-temperature diagram of the piracetam system. The experimental triple points are reported from 1 to 5. Solid black circles 1 and 4 are stable triple points, solid grey circles are triple points of lower stability than points 1 and 4, and empty circles are triple points of lower stability than the solid grey triple points. The triple points where the vapor phase is involved are: (1) I-liquid-vapor, (2) II-liquid-vapor, (3) III-liquid-vapor, (4) III-I-vapor, and (5) II-I-vapor. Inset: zoom of the lower part of the diagram. For clarity: the melting curves of Forms II and III are represented in red, the III-I and II-I equilibrium lines in blue, and the sublimation curves of Forms III and II in green.

Since the studied system is trimorphic, ten triple points as well as ten two-phase equilibria have to be considered for the construction of the p-T phase diagram [24]. Because Form III is the most stable solid form at low temperature, the III-I-vapor triple point is stable (figure 3, point 4) and located on the I-vapor equilibrium line. The transition point between Forms II and I, *i.e.* the II-I-vapor triple point (point 5 in Figure 3), is also located on the I-vapor equilibrium line but at a lower temperature than the III-I-vapor triple point (table 4). The latter triple point 5 is necessarily metastable compared to the III-I-vapor one. The overestimated melting enthalpy value of Form II leads to a melting slope equal to 4.38 MPa K^{-1}. Although higher than the possible true value, this value remains lower than the melting slope value of Form I.

Since $\frac{dP}{dT}(II-liquid) < \frac{dP}{dT}(III-liquid) < \frac{dP}{dT}(I-liquid)$, it follows that: i/ the II-liquid equilibrium line will intersect the I-liquid equilibrium one at point 6 in figure 3, located below the intersection between III-liquid with I-liquid equilibrium curves (point 7 in figure 3), ii/ the II-liquid and III-liquid equilibrium curves will intersect at a temperature and a pressure above points 6 and 7 in figure 3 (point 8). Point 8 is located in the liquid phase region, accordingly to the lower slopes of II-liquid and III-liquid compared to the I-liquid one.

Since the II-I equilibrium line has to pass through point 6 (II-I-liquid triple point) and the III-I equilibrium line has to pass through point 7 (III-I-liquid triple point), the II-I and III-I equilibrium lines will intersect at a temperature and a pressure above the triple points 4 and 5 (point 9 of figure 3). This point is the III-II-I triple point. As seen on the phase diagram, since the II-I equilibrium line passes through points 5 and 6 and the III-I equilibrium line through points 4 and 7, the slope of the II-I equilibrium line is necessary lower than that of the III-I equilibrium one. According to the calculated slopes (table 7), this should have been the opposite, although very close values. But the calculation gives the slope at the origin with the approximation that the two-phase equilibrium curve is treated as a straight line. This is not completely true and may explain the disagreement between the calculation and the thermodynamic construction.

The sublimation curves of Forms III and II have to pass through points 4 and 3 and points 2 and 5 respectively. Both equilibria (green lines in figure 3) will intersect just above point 4 to give the tenth triple point III-II-vapor (see inset in figure 3). This implies that Forms III and II are enantiotropes of each other, as previously concluded [11].

Since the I-liquid equilibrium is stable between points 1 and 6, point 6 becomes a stable triple point. Then, below point 6, the I-L equilibrium is stable when, above this point, the II-liquid equilibrium becomes stable. As a consequence, the III-I-liquid triple point (point 8) becomes stable. Alternatively around point 8, the III-liquid equilibrium becomes stable at high temperature and pressure when the II-liquid equilibrium becomes stable down to point 9 which, consequently, becomes stable.

Keeping in mind that, when turning around a triple point, we go through curves which represent alternately the coexistence of two states of greater stability than the next two [25], and since a triple point is the common point of three two-phase equilibrium curves, the plane

around this point is divided into six parts [25]. If one of the two-phase equilibrium curves is stable, then the triple point is necessarily stable, and we have to find two other stable two-phase equilibrium curves around this point. On this basis, since points 4 (III-I-vapor) and 9 (III-II-I) are stable triple points, the III-I equilibrium is necessarily stable between those two points. The third two-phase equilibrium between points 6 and 9 is then necessarily stable.

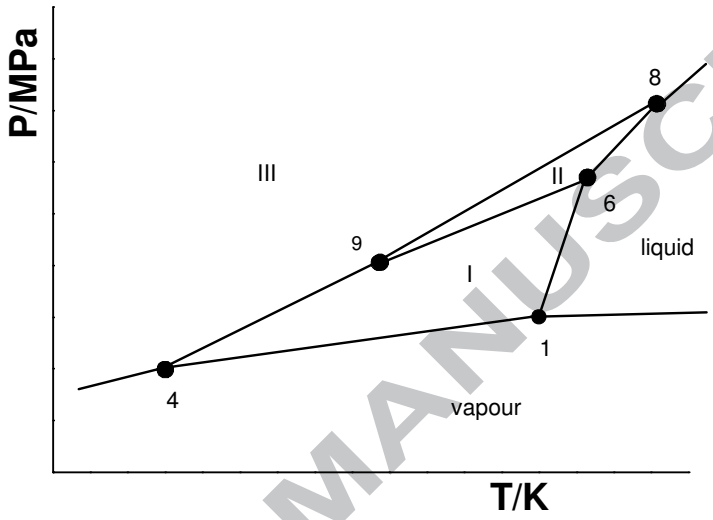

FIGURE 4. Schematic phase diagram of the piracetam system, presenting the stability domain of the three polymorphs as well as the liquid and vapor phases, as a function of temperature and pressure.

Taking into account all the above results, the resulting equilibrium phase diagram is presented in Figure 4, where five stable triple points are identified. From this diagram, it clearly appears that Form II is stable under pressure since its domain of stability is located just above that of Form I. If the pressure exerted becomes stronger, then Form II transits into Form III. This diagram also reveals that, on heating and depending on the pressure exerted on the system, Form III could transform into Form I or Form II before melting, or can melt directly when the pressure is very high (*i.e.* for an exerted pressure higher than the equilibrium pressure of point 8).

4. Conclusion

Most of the values obtained from this work are lower than those already published, probably due to the fact that the transition points are heating scan-rate dependent.

The molar volumes in the solid state measured for Forms II and III from ambient temperature to the transition temperature, although very close, show that Form III is always denser than Form II in this range of temperature. This remains true down to 0 K, since Form II molar volume is found to extrapolate at V = 97.6 cm^3 mol^{-1} and Form III at 96.7 cm^3 mol^{-1}. The new phase diagram clearly establishes that the stability domain of Form II is very small and located just above the stability domain of Form I. Under pressure, the diagram shows that Form I may transform into Form II and then, still increasing the pressure, Form II should transform into Form III.

5. Final remarks

Since no thermodynamic data are available for Forms IV and V, it was not possible to locate their stability domain in the p-T phase diagram. However, since Form V is obtained from direct compression of Form II, it is highly probable that the stability domain of Form V is located on the upper part of the diagram, somewhere above the stability domain of Form II. As far as Form IV in concerned, this phase is not obtained by direct compression of any other phase(s). So it is more difficult to try to set the stability domain of this phase in the p-T phase diagram, even if this phase is located in the high-pressure domain. Anyway, since Forms IV and V are high-pressure phases, it is likely that they do not alter the stability domains of Forms I and II. Moreover, the stability domain of Form III will remain unchanged even for medium pressures. Nevertheless, when an external pressure is exerted on the raw material during the manufacture of tablets, for instance, a polymorphic transformation may occur. In the case of piracetam Form III, one cannot exclude a III toward IV or a III toward V transformation, although that has never been observed experimentally.

Acknowledgements

This work was financially supported by the ANR project NPLIN-4-drug (1 year postdoctoral position of C. A.). Ms. K. Debbasch is kindly thanked for her advice on the manuscript, and Dr I. Nicolis for fruitful discussions on the probability laws.

References

[1] G. Bandoli, D.A. Clemente, A. Grassi, G.C. Pappalardo, Pharmacol. 20 (1981) 558-564.

[2] G. Admiraal, J.C. Eikelenboom, A.Vos, Acta Crystallogr. B 38 (1982) 2600-2605.

[3] M. Kuhnert-Brandstätter, A. Burger, R. Völlenklee, Sci. Pharm. 62 (1994) 307-316.

[4] R. Céolin, V. Agafonov, D. Loüer, V.A. Dzyabchenko, S. Toscani J.M. Cense, J. Sol. State Chem. 122 (1996) 186-194.

[5] F.P.A. Fabbiani, D.R. Allan, S. Parsons, C.R. Pulham, CrystEngComm. 7 (2005) 179-186.

[6] F.P.A. Fabbiani, D.R. Allan, W.I.F. David, A.J. Davidson, A.R. Lennie, S. Parsons, C.R. Pulham, J.E. Warren, Cryst. Growth Des. 7 (2007) 1115-1124.

[7] R. Picciochi, H.P. Diogo, M.E. Minas de Piedade, J. Pharm. Sci. 100 (2011) 594-603.

[8] D. Louër, M. Louër, V.A. Dzyabchenko, V. Agafonov, R. Céolin, Acta Crystallogr. B51 (1995) 182-187.

[9] A. Maher, D.M. Croker, C.C. Seaton, A.C. Rasmuson, B.K. Hodnett, Cryst. Growth Des. 14 (2014) 3967-3974.

[10] A. Maher, A.C. Rasmuson, D.M. Croker, B.K. Hodnett, J. Chem. Eng. Data 57 (2012) 3525-3531.

[11] A. Maher, C.C. Seaton, S.Hudson, A.C. Croker, D.M. Rasmuson, B.K. Hodnett, Cryst. Growth Des. 12 (2012) 6223-6233.

[12] P.L.D. Wildfong, Effects of pharmaceutical processing on the soid form of drug and excipient materials, in: H.G. Brittain (Ed.), Polymorphism in pharmaceutical solids, Informa Healthcare, New York, 2009; pp 510-559.

[13] J.F. Bérar, G. Calvarin, D. Weigel, J. Appl. Cryst. 13 (1980) 201-206.

[14] V. Swamy, N.A. Dubrovinskaya, L.S. Dubrovinsky, J. Mater. Res. 14 (1999) 456-459.

[15] V. Petricek, M. Dusek, L. Palatinus, Z. Kristallogr. 229 (2014) 345-352.

[16] Y. Corvis, M-C. Menet, P. Négrier, P. Espeau. New J. Chem. 37 (2013) 761-768.

[17] W. Ostwald, Z. Phys. Chem. 22 (1897) 289-330.

[18] A.I. Kitaigorodskii, Molecular crystals and molecules, Academic press, New York, 1973.

[19] P.J. Sinko, Martin's physical pharmacy and pharmaceutical sciences, sixth ed., Lippincott Williams & Wilkins, Philadelphia, 2011, pp 61-62.

[20] A. Burger, R. Ramberger, Microchim. Acta [Wien] (1979) 259-271.

[21] P. Espeau, R. Céolin, J.L. Tamarit, M.A. Perrin, J.P. Gauchi, F. Leveiller, J. Pharm. Sci. 94 (2005) 524-539.

[22] P. Espeau, P. Négrier, Y. Corvis, Cryst. Growth Des. 13 (2013) 723-730.

[23] P. Espeau, R. Céolin, Thermochim. Acta 376 (2001) 147-154.

[24] E. Riecke, Z. Phys. Chem. 6 (1890) 411-429.

[25] J. W. Gibbs, Trans. Conn. Acad. Arts Sci. 3 (1876) 108-248.

Highlights

- Thermal analyses and X-ray diffraction experiments are performed.
- Scan-rate dependence of the transition points is highlighted.
- A new phase diagram of piracetam is proposed.
- The new hierarchy of polymorphs stability is now coherent with all published data.